Observation of the quantum interference phenomenon induced by interacting dark resonances

Ying-Cheng Chen, Yean-An Liao, Hsin-Ying Chiu, Jung-Jung Su, and Ite A. Yu
Department of Physics, National Tsing Hua University, Hsinchu, Taiwan 300, Republic of China
(Received 12 June 2001; published 2 October 2001)

We report an experimental observation of narrow and high-contrast spectra, which are induced by interacting dark resonances and have been predicted in Phys. Rev. A **60**, 3225 (1999). Spectra are measured with cold ^{87}Rb atoms produced by a magneto-optical trap. In this experimental system, a coupling laser and a weak probe laser form a three-level Λ-type configuration of electromagnetically induced transparency (EIT); a microwave drives a magnetic-dipole transition between the fourth level and the ground state that is coupled with the excited state by the coupling laser. The observed spectral profile of probe absorption exhibits a very sharp peak emerging inside a narrow EIT dip. Such spectral feature provides more opportunities in manipulating atomic-optical response.

DOI: 10.1103/PhysRevA.64.053806 PACS number(s): 42.50.Gy, 42.62.Fi, 32.80.Pj

The phenomena of electromagnetically induced transparency (EIT) and coherent population trapping [1–7] have made possible many interesting and important progresses of manipulating atomic-optical responses. For examples, a light pulse is slowed down significantly or even trapped in an atomic medium [8–11]; lasing occurs without population inversion [12,13]; atoms are laser cooled below the recoil limit [14]. Existence of the dark resonance in a three-level system, formed by two ground states and an excited state driven by two laser fields, is the basis of these phenomena. Recently, an intriguing proposal in Ref. [15] predicts that interference between two dark resonances in a four-level system can further enhance the degree of freedom in manipulating atomic-optical responses. In the four-level system, a coupling laser and a weak probe laser form a three-level Λ-type configuration of EIT; a microwave drives a magnetic-dipole transition between the fourth level and the ground state that is coupled with the excited state by the coupling laser. Our experimental study is intended for observation of the interference phenomenon induced by the two interacting dark resonances (IDR). This observation has not been reported before.

We present a simple physical picture about the IDR phenomenon. The four-level system is shown in Fig. 1(b). We can view this system in the basis dressed by the microwave. Since the microwave only couples the states $|c\rangle$ and $|d\rangle$, superposition of $|c\rangle$ and $|d\rangle$ form the dressed states [say $|1(N)\rangle$ and $|2(N)\rangle$]. $|a\rangle$ and $|b\rangle$ are intact in the dressed-state basis. In the spectroscopic measurement with the coupling frequency fixed and the probe frequency scanned, we should observe two dark resonances or transparency lines of probe absorption when the coupling and probe frequencies satisfy the two-photon resonance conditions from $|b\rangle$ to $|1(N)\rangle$ and from $|b\rangle$ to $|2(N)\rangle$. For the two-photon transition that starts from $|b\rangle$ and ends in the middle of $|1(N)\rangle$ and

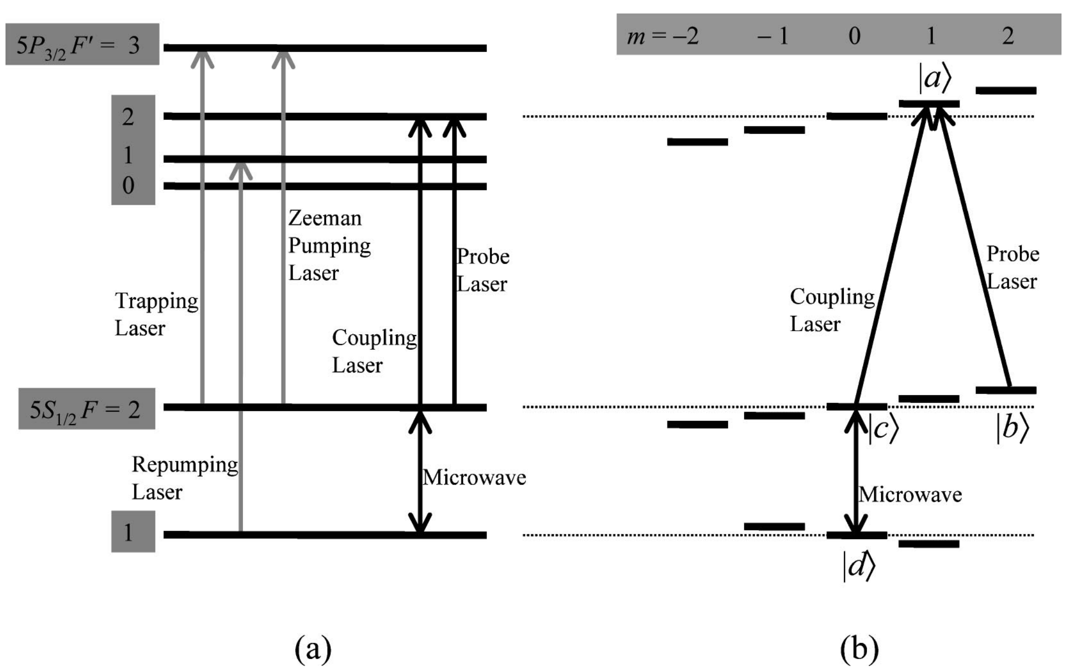

FIG. 1. (a) Relevant energy levels of ^{87}Rb atoms and excitations of the laser and microwave fields in the experiment. (b) The four-level system in the experiment.

$|2(N)\rangle$, interference between the two dark lines results in an absorption peak. An IDR spectral profile will exhibit three absorption peaks with two in-between transparency dips. The two transparency dips and the central peak in the IDR spectrum can be very narrow and of high contrast. Some interesting applications of such spectral features and details of the IDR phenomenon have been discussed in Ref. [15] and we will not repeat them here.

We measure the IDR spectra in cold ^{87}Rb atoms produced by a vapor-cell magneto-optical trap (MOT) [16,17]. Our MOT has been described elsewhere and we only mention some essential points that differ from the MOT setup in Ref. [18]. The repumping beam drives the $|5S_{1/2},F=1\rangle \rightarrow |5P_{3/2},F'=1\rangle$ transition resonantly. It has an $1/e$ diameter of 10 mm and a power of 8 mW. Both trapping and repumping beams can be switched off by acousto-optic modulators (AOM). A solid-state relay connects the anti-Helmholtz magnet and a power supply. When the relay is being turned off, decay time constant of current in the magnet is about 30 μs. All laser and magnetic fields of the MOT are not present during the spectrum measurement. Typically, we trap 4×10^7 atoms with a temperature of 250 μK in the MOT.

The coupling and probe beams come from two diode lasers. They drive the $|5S_{1/2},F=2\rangle \rightarrow |5P_{3/2},F'=2\rangle$ transition of ^{87}Rb atoms as shown in Fig. 1. (The notation of F will indicate the $|5S_{1/2}\rangle$ ground state and that of F' will indicate the $|5P_{3/2}\rangle$ excited state.) Both coupling and probe lasers are injection locked by the same master, which is an external-cavity diode laser with a linewidth narrower than 1 MHz. One beam from the master laser is sent through an AOM and the diffracted output beam from the AOM seeds the coupling laser. We adjust driving frequency of the AOM to change the coupling frequency. Another beam from the master laser is sent through another AOM in the double-pass configuration. The twice-diffracted output beam from this AOM seeds the probe laser. Driving frequency of the AOM is modulated during the spectrum measurement to sweep the probe frequency. This double-pass configuration ensures that the optical alignment of the injection locking of the probe laser remains unchanged when the probe frequency is swept. The beat signal between the coupling and probe lasers shows a spectral linewidth below 1 kHz. Before the two laser beams interact with atoms, each of them passes through an AOM and can be individually switched on or off. We keep the driving frequencies of these two AOMs constant through the entire experiment. The coupling and probe fields are circularly polarized with right (σ_+ polarization) and left (σ_- polarization) helicities, respectively. They propagate nearly in the same direction with an angle separation below 1°. We denote this direction as the z axis.

We apply a 6.8-GHz microwave to drive the magnetic-dipole transition between $|F=1\rangle$ and $|F=2\rangle$. The microwave comes from a homemade antenna to which we deliver a power of 37 dBm. We build and orient the antenna such that magnetic field of the antenna output is linearly polarized and its polarization direction close to the z axis. Frequency fluctuation of the microwave is less than 10 Hz. A microwave spectroscopy is employed to determine frequency and

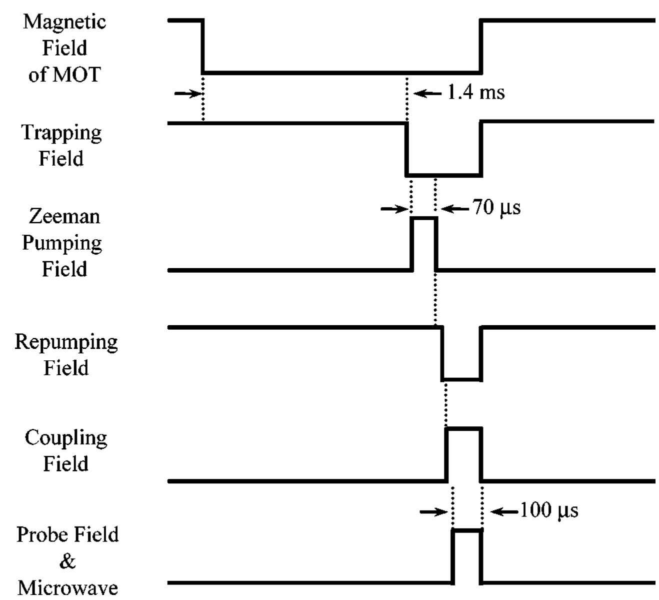

FIG. 2. The timing sequence of the measurement of the IDR spectra. This sequence is repeated at a period of 12 ms.

intensity of the microwave. In the spectroscopy, all population of the cold atoms is optically pumped to the $|F=1\rangle$ state. Then, the microwave is turned on for 1 ms without the presence of the MOT fields and any other laser fields. At the end of the microwave pulse, we detect the population in the $|F=2\rangle$ state. This measurement sequence is periodically repeated and frequency of the microwave is slowly scanned. A small dc magnetic field is applied to separate different transitions. Positions and widths of transition lines in the microwave spectrum provide information about the microwave field.

Three pairs of Helmholtz magnets are installed to cancel stray magnetic field from the environment. An additional dc magnetic field of 0.6 G is applied in the z axis. This dc magnetic field separates the desired four-level system from unwanted microwave transitions. In the four-level system, the σ_- probe drives $|F=2,m=2\rangle \rightarrow |F'=2,m=1\rangle$ transition, the σ_+ coupling drives $|F=2,m=0\rangle \rightarrow |F'=2,m=1\rangle$ transition, and the microwave drives $|F=1,m=0\rangle \rightarrow |F=2,m=0\rangle$ transition as shown in Fig. 1(b). We will use $|a\rangle$, $|b\rangle$, $|c\rangle$, and $|d\rangle$ to indicate the $|F'=2,m=1\rangle$, $|F=2,m=2\rangle$, $|F=2,m=0\rangle$, and $|F=1,m=0\rangle$ states, respectively.

The timing sequence of the IDR-spectrum measurement is shown in Fig. 2. We first turn off the magnetic field of the MOT. 1.4 ms later, the trapping beams are shut off. The 1.4-ms delay prevents measured spectra from influence of the MOT magnetic field. A Zeeman pumping beam is switched on for 70 μs with an AOM. It drives $|F=2\rangle \rightarrow |F'=3\rangle$ transition resonantly with σ_+ polarization and an intensity of 0.6 mW/cm^2. This Zeeman pumping beam as well as the repumping beam of the MOT prepares population in the $|b\rangle$ state. After we turn off the two pumping beams, the coupling, probe, and microwave fields are switched on for about 100 μs. At the end of this 100 μs, all MOT fields return. The above sequence is repeated at a period of 12 ms. Absorption of the probe field is detected by a photodiode.

Output of the photodiode is sent to a lock-in amplifier. The lock-in amplifier generates spectra and its reference signal is the pulse switching the probe beam. Spectra are measured in the way that the coupling and microwave frequencies are fixed and the probe frequency is slowly swept. We typically sweep the probe frequency at a speed of 600 kHz/s. Such a method of short pulse and slow sweep can minimize deformation or asymmetry of spectra caused by forces from the laser beams or population loss of the $|b\rangle$ state.

In order to analyze experimental data, we calculate probe-absorption spectra by solving the optical Bloch equation of density-matrix operator described in the following:

$$\frac{d\rho}{dt}=\frac{1}{i\hbar}[H_{\rm atom}+H_{\rm coupling}+H_{\rm microwave}+H_{\rm probe},\rho]+\left\{\frac{d\rho}{dt}\right\}. \tag{1}$$

$H_{\rm atom}$ is the atom Hamiltonian. $H_{\rm coupling}$, $H_{\rm microwave}$, and $H_{\rm probe}$ are the Hamiltonians of the coupling, microwave, and probe fields in the rotating-wave approximation. $\{d\rho/dt\}$ describes relaxation of ρ and its elements as

$$\left\{\frac{d}{dt}\rho_{aa}\right\}=-(\Gamma_b+\Gamma_c+\Gamma_d)\rho_{aa},$$

$$\left\{\frac{d}{dt}\rho_{bb}\right\}=\Gamma_b\rho_{aa},\quad \left\{\frac{d}{dt}\rho_{cc}\right\}=\Gamma_c\rho_{aa},$$

$$\left\{\frac{d}{dt}\rho_{dd}\right\}=\Gamma_d\rho_{aa}, \tag{2}$$

$$\left\{\frac{d}{dt}\rho_{ij}\right\}=-\Gamma_{ij}\rho_{ij}, \tag{3}$$

with

$$\Gamma_{ab}=\frac{\Gamma_b}{2},\quad \Gamma_{ac}=\frac{\Gamma_c}{2},\quad \Gamma_{ad}=\frac{\Gamma_d}{2},\quad \Gamma_{bc}=\Gamma_{bd}=\Gamma_{cd}=\gamma.$$

In the above equations, Γ_b, Γ_c, and Γ_d are the spontaneous decay rates from $|a\rangle$ to $|b\rangle$, $|c\rangle$, and $|d\rangle$, respectively; γ is the relaxation rate of coherence between the ground states. We assume γ is negligible when it is compared to any of the spontaneous decay rates. Treating the weak $H_{\rm probe}$ as a perturbation, we carry out the calculation to all orders of $H_{\rm atom}+H_{\rm coupling}+H_{\rm microwave}$ and to the first order of $H_{\rm probe}$. After the stationary solution of Eq. (1) is found numerically, the probe absorption is proportional to the imaginary part of the amplitude of ρ_{ab}. Our calculation results are consistent with the predictions in Ref. [15].

In the absence of the microwave field, widths of EIT dips are about 70 kHz at a contrast of 80% and 40 kHz at a contrast of 60%. Contrast is defined as (maximum $-$minimum)/(maximum$+$minimum) of the dip in the probe-absorption spectrum. Comparing these observations with theoretical predictions, we estimate that the relaxation rate γ in Eq. (3) is around 0.002Γ in our system, where $\Gamma=2\pi\times5.9$ MHz is the spontaneous decay rate of the $|5P_{3/2}\rangle$ excited states. To achieve this level of γ, the delay time between shutting off the MOT magnet and turning on the fields for the spectroscopy is an important factor. It should be long enough. This is because we observe magnetic induction of the environment induced by the MOT field decays rather slowly although current of the MOT magnet can be turned off quickly. On the other hand, improperly long delay time will degrade the number of atoms and hinder the spectroscopic measurement. Phase lock between the coupling and probe fields is another important factor. Laser-linewidth effects are eliminated in this situation [19]. Otherwise, phase fluctuations of the laser fields will contribute to γ greatly.

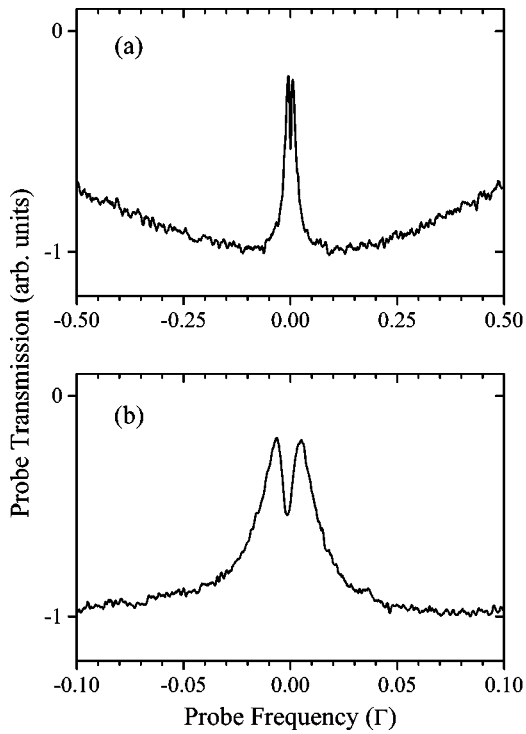

FIG. 3. Experimental IDR spectra. 0 in all vertical axes indicates no absorption. (a) and (b) are measured in the same conditions except that the sweep rate of the probe field is reduced to 120 kHz/s in (b). A slower sweep rate reveals the actual IDR peak height.

From the theoretical calculation, the IDR phenomenon can only be observed under a small γ. When the microwave field is applied, a very sharp absorption peak emerges in the EIT dip as the spectra shown in Fig. 3. Such spectral profile is an evidence of the quantum-interference effect induced by IDR. Presence of the microwave field creates two dark lines whose resonances correspond to the two transparency points in the spectra. Interference between the two dark lines leads to the central peak, which can also be viewed as the three-photon resonance from $|b\rangle$ to $|d\rangle$. For the data shown in Fig. 3, the coupling and microwave fields are resonant and their Rabi frequencies are $\Omega_c\approx0.2\Gamma$ and $\Omega_m\approx0.012\Gamma$, respectively. We measure Ω_c from separation of the two absorption peaks in the EIT spectrum. Ω_m is determined from the microwave spectroscopy in which linewidth of the $|d\rangle$ to $|c\rangle$ transition is dominantly due to power broadening. Although we have delivered a maximum power of 37 dBm to the microwave antenna and made efforts to optimize the antenna's

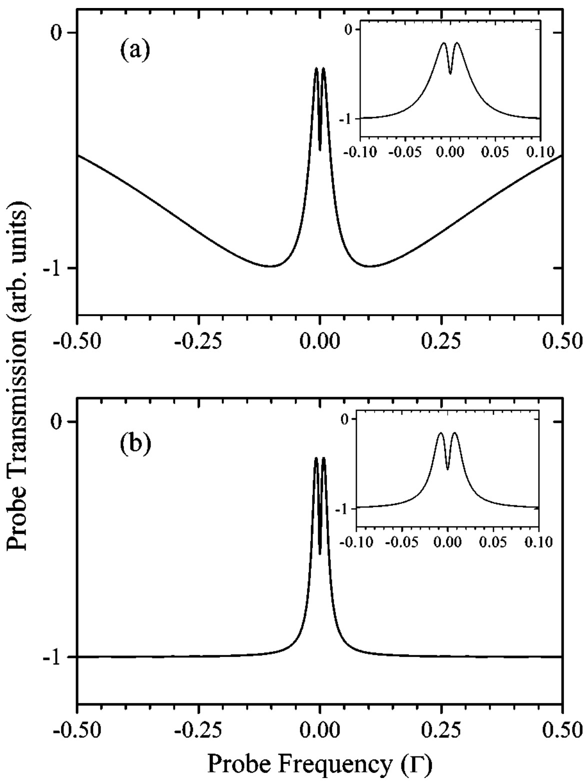

FIG. 4. Theoretical IDR spectra of cold atoms in (a) and room-temperature atoms in (b). 0 in all vertical axes indicates no absorption. Inset displays the same spectrum in a smaller range. Ω_c used in (b) is eight times of that used in (a). In (b), we evaluate the velocity groups with respect to the Doppler shifts from -100Γ to 100Γ.

structure and position, the Rabi frequency received by the atoms is still small. Figure 4(a) shows the spectrum from the theoretical calculation. In the calculation, we use $\Omega_c = 0.2\Gamma$, $\Omega_m = 0.012\Gamma$, and $\gamma = 0.002\Gamma$. The agreement between the experimental data and the theoretical prediction is satisfactory.

We make a few notes about observing IDR spectra.

(i) The central peak height in the IDR spectrum is very sensitive to dc magnetic fields in the transverse directions or the xy plane. A transverse field of 0.01 G significantly reduces the IDR peak. Larmor precession induced by the transverse field may deteriorate ground-state coherence and cause the problem. Because the Rabi frequency of the coupling field is large, the EIT window is influenced little by this small transverse field. The observation indicates that the IDR peak can be a sensitive detector for transverse magnetic fields. Further investigation is required to quantitatively clear the issue.

(ii) If the coupling Rabi frequency is too small, the EIT window will be too narrow to observe the IDR peak. On the other hand, if the coupling Rabi frequency is too large, the IDR peak will also be degraded. This is because light shift of the $|c\rangle$ state induced by the coupling field increases the detuning of the microwave field and the three-photon transition rate from $|b\rangle$ to $|d\rangle$ decreases. The statement is also supported by the observation that adding a small detuning to the microwave field reduces the IDR peak height.

(iii) Figure 4(b) shows a theoretical IDR spectrum of room-temperature ^{87}Rb atoms. Spectra from all different velocity groups are summed up to give the result. In the calculation, we use $\Omega_c = 1.6\Gamma$, $\Omega_m = 0.012\Gamma$, and $\gamma = 0.002\Gamma$ and assume that the coupling and probe fields propagate in the exactly same direction. Since EIT dips are narrower and shallower for room-temperature samples, a larger coupling Rabi frequency should be applied such that IDR peaks of room-temperature atoms will be as observable as those of cold atoms.

A recent publication reports experimental spectra of doubly dressed states in cold atoms [20]. The four-level system in their study is similar to ours except that $|d\rangle$ is an excited state. Their spectrum shows an absorption peak emerging inside the Autler-Townes doublet due to presence of a pump laser driving the optical transition between $|c\rangle$ and $|d\rangle$. Reference [21] has predicted that this pump field can be used to completely switch off the EIT effect. We further point out that linewidth of the central peak in Ref. [20] cannot be narrower than the natural linewidth of the excited $|d\rangle$ state. Although theoretical treatments of their doubly-dressed system and our IDR system can be similar, experimental outcomes and potential applications of the two systems are different.

In conclusion, we have experimentally demonstrated the high-contrast and narrow-linewidth spectra induced by interacting dark resonances. The observations are in agreement with the theoretical predictions. Important experimental factors in observing the IDR phenomenon have been studied and reported. Our work opens an avenue of manipulating atomic-optical response via the IDR system. We anticipate that some interesting applications of the IDR system will be further pursued.

This work is supported by the National Science Council of the Republic of China under NSC Grant No. 89-2112-M-007-061. We are grateful to Professor Jow-Tsong Shy for loaning us the microwave instruments that were partially key to the success of this work.

[1] E. Arimondo and G. Orriols, Lett. Nuovo Cimento **17**, 333 (1976).
[2] G. Alzetta, A. Gozzini, L. Moi, and G. Orriols, Nuovo Cimento Soc. Ital. Fis., B **36B**, 5 (1976).
[3] H. M. Gray, R. M. Whitley, and C. R. Stroud, Jr., Opt. Lett. **3**, 218 (1978).
[4] For a review of coherent population trapping, see E. Arimondo, in *Progress in Optics XXXV*, edited by A. Wolf (Elsevier, Amsterdam, 1996), p. 258.
[5] A. Imamoğlu and S. E. Harris, Opt. Lett. **14**, 1344 (1989).
[6] K. J. Boller, A. Imamoğlu, and S. E. Harris, Phys. Rev. Lett. **66**, 2539 (1991).

[7] For a review of electromagnetically induced transparency, see S. E. Harris, Phys. Today **50** (7), 36 (1997).
[8] L. V. Hau, S. E. Harris, Z. Dutton, and C. H. Behroozi, Nature (London) **397**, 594 (1999).
[9] D. Budker, D. F. Kimball, S. M. Rochester, and V. V. Yashchuk, Phys. Rev. Lett. **83**, 1767 (1999).
[10] C. Liu, Z. Dutton, C. H. Behroozi, and L. V. Hau, Nature (London) **409**, 490 (2001).
[11] D. F. Phillips, A. Fleischhauer, A. Mair, R. L. Walsworth, and M. D. Lukin, Phys. Rev. Lett. **86**, 783 (2001).
[12] O. A. Kocharovskaya and Ya. I. Khanin, Pis'ma Zh. Eksp. Teor. Fiz. **48**, 581 (1998) [JETP Lett. **48**, 630 (1988)].
[13] G. G. Padmabandu, G. R. Welch, I. N. Shubin, E. S. Fry, D. E. Nikonov, M. D. Lukin, and M. O. Scully, Phys. Rev. Lett. **76**, 2053 (1996).
[14] A. Aspect, E. Arimondo, R. Kaiser, N. Vansteenkiste, and C. Cohen-Tannoudji, Phys. Rev. Lett. **61**, 826 (1988).
[15] M. D. Lukin, S. F. Yelin, M. Fleischhauer, and M. O. Scully, Phys. Rev. A **60**, 3225 (1999).
[16] E. L. Raab, M. Prentiss, A. Cable, S. Chu, and D. E. Pritchard, Phys. Rev. Lett. **59**, 2631 (1987).
[17] C. Monroe, W. Swann, H. Robinson, and C. Wieman, Phys. Rev. Lett. **65**, 1571 (1990).
[18] Y. C. Chen, Y. W. Chen, J. J. Su, J. Y. Huang, and I. A. Yu, Phys. Rev. A **63**, 043808 (2001).
[19] B. J. Dalton and P. L. Knight, J. Phys. B **15**, 3997 (1982).
[20] M. Yan, E. G. Rickey, and Y. Zhu, Phys. Rev. A **64**, 013412 (2001).
[21] S. E. Harris and Y. Yamamoto, Phys. Rev. Lett. **81**, 3611 (1998).